Supporting Information

Novel $\alpha_v\beta_3$ Integrin-Targeted NIR-II Nanoprobe for Multimodal Imaging-guided Photothermal Therapy of Tumor *In Vivo*

Meng Zhao,[a] Jianan Ding,[a] Qiulian Mao,[a] Yuqi Zhang,[a] Yinjia Gao,[a] Shuyue Ye,[a] Hongni Qin[b] and Haibin Shi[a,*]

[a] State Key Laboratory of Radiation Medicine and Protection, School for Radiological and Interdisciplinary Sciences (RAD-X) and Collaborative Innovation Centre of Radiation Medicine of Jiangsu Higher Education Institution, Soochow University, Suzhou 215123, P. R. China

[b] Suzhou Industrial Park Institute of Services Outsourcing, Suzhou 215123, Jiangsu, P. R. China

[*]Corresponding author: hbshi@suda.edu.cn

1. Materials

3-bromoprop-1-yne, cyclohexanone, 4-mercaptophenol and methylmagnesium chloride (3.0 M solution in tetrahydrofuran (THF)) were provided by Energy Chemical (Shanghai, China). Ethyl-3-bromopropanoate, benzo[*cd*]indol-2(1*H*)-one and potassium hexafluorophosphate were purchased from Aladdin (Shanghai, China). Phosphorus oxychloride, sodium acetate and acetic anhydride were purchased from Sinopharm Chemical Reagents (Shanghai, China). cRGD-N_3 was synthesized by GL Biochem (Shanghai, China) as requested. Radionuclide ($Na^{125}I$) was obtained from GMS Pharmaceutical Co. Ltd (Shanghai, China). All other chemicals were of analytical grade obtained from Sinopharm Chemical Reagents (Shanghai, China). All the chemicals were of reagent-grade and used without further purification.

2. Characterizations

^{1}H-NMR spectra were recorded on a Bruker Advance III 400 MHz spectrometer, and ^{13}C-NMR spectra were recorded on 100 MHz spectrometers at 25 °C. The chemical shifts were reported as parts per million from tetramethylsilane (TMS, $\delta = 0$). Mass spectra were determined with an Ultraflextreme MALDI TOF/TOF. The UV-visible NIR absorption spectra were measured on a PerkinElmer LAMBDA 750 spectrophotometer. The NIR-II fluorescence emission spectra were performed on an Edinburgh FLS980 spectrophotometer with 808 nm laser diode. The HPLC profiles were acquired on Agilent 1260 high performance liquid chromatography. Dynamic light scattering (DLS) measurements were carried out on a particle size analyzer (Nano ZS90, Malvern) at room temperature. The TEM images were taken under an electron microscope (Tecnai G2 Spirit, FEI).

3. Synthesis of compounds

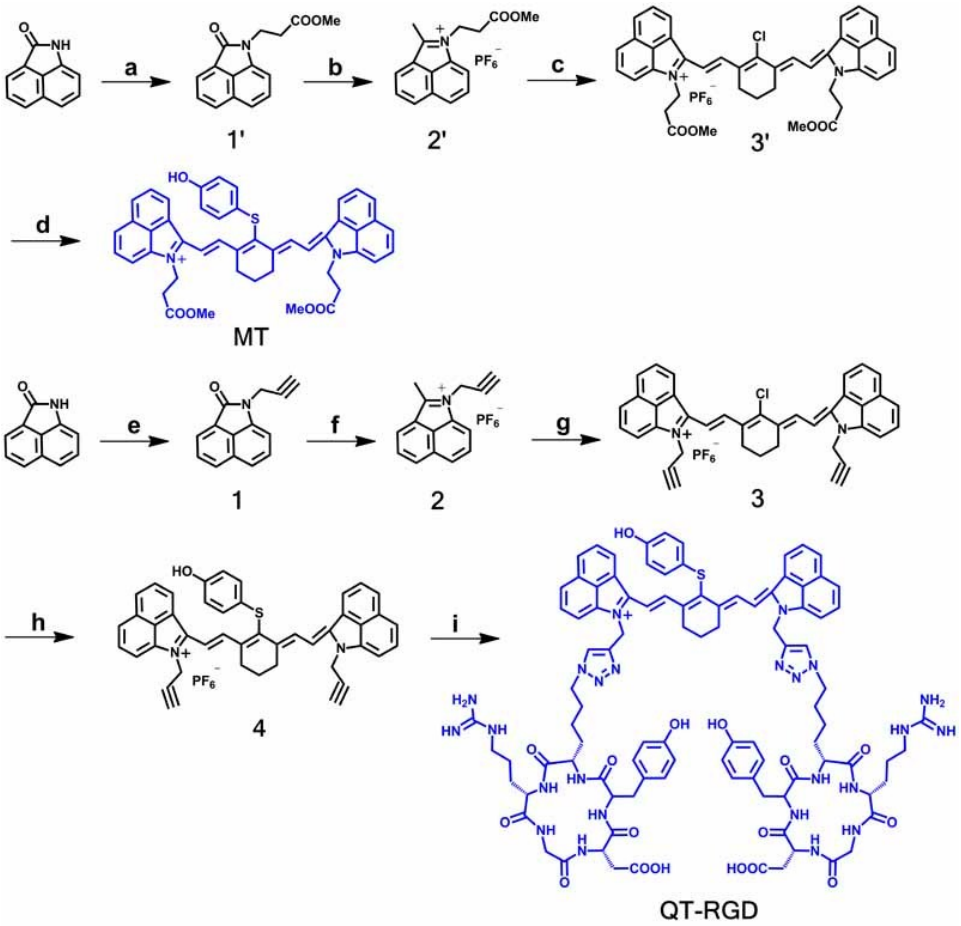

Scheme S1. Schematic representation of the synthesis procedure of probes MT and QT-RGD. (a) $BrCH_2CH_2COOMe$, K_2CO_3, DMF, 100°C, 18 hours; (b) MeMgCl, tetrahydrofuran, KPF_6, 70°C, 3 hours; (c) 2-chloro-3-(hydroxymethylene)cyclohex-1-enecarbaldehyde, CH_3COONa, $(CH_3CO)_2O$, 40°C, 2 hours; (d) 4-mercaptophenol, DMF, 25°C, 4 hours; (e) $BrCH_2CCH$, K_2CO_3, DMF, 100°C, 18 hours; (f) MeMgCl, tetrahydrofuran, KPF_6, 70°C, 3 hours; (g) 2-chloro-3-(hydroxymethylene)cyclohex-1-enecarbaldehyde, CH_3COONa, $(CH_3CO)_2O$, 40°C, 2 hours; (h) 4-mercaptophenol, DMF, 25°C, 4 hours; (i) cRGD-N_3, $CuSO_4 \cdot 5H_2O$, sodium ascorbate, 25°C, 2 hours.

Synthesis of compound 1'. Compounds benzo[cd]indol-2(1H)-one (2.53 g, 15.0 mmol) and methyl-3-bromopropanoate (7.52 g, 45.0 mmol) were dissolved in N,N-dimethyformamide (80.0 mL) under nitrogen and with constant stirring, the solution was refluxed for 6 hours. Then the mixture was poured into a large amount of ice water and adjusted to pH 7~8 with 1 M hydrochloric acid solution. The precipitate produced

was filtered under suction, which was further purified by column chromatography using petroleum ether/ethyl acetate (9:1, v/v) as the eluent to give compound 1' as yellow oil with a yield of 78% (3.14 g).

^{1}H-NMR (d_6-DMSO, 400 MHz, ppm) δ = 8.20 (d, J = 8.1 Hz, 1H), 8.06 (d, J = 7.0 Hz, 1H), 7.81 (t, J = 7.6 Hz, 1H), 7.65 (d, J = 8.4 Hz, 1H), 7.56 (t, J = 7.7 Hz, 1H), 7.24 (d, J = 7.0 Hz, 1H), 4.16 (t, J = 7.0 Hz, 2H), 3.54 (s, 3H), 2.79 (t, J = 7.0 Hz, 2H). ^{13}C-NMR (d_6-DMSO, 100 MHz, ppm) δ = 171.77, 167.28, 138.91, 131.57, 129.38, 129.36, 129.13, 126.16, 124.74, 124.50, 120.55, 106.33, 51.93, 36.40, 33.19. MALDI-MS: Calcd. For $C_{15}H_{14}NO_3^+$ [M+H$^+$] 256.097, *found*: 256.293.

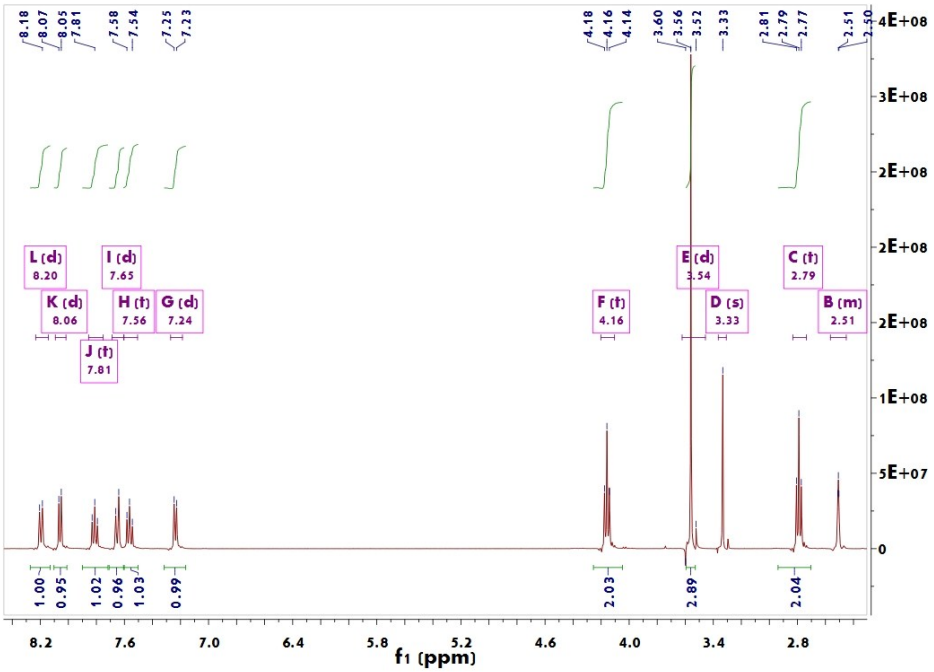

Fig. S1. ^{1}H-NMR spectra of compound 1'.

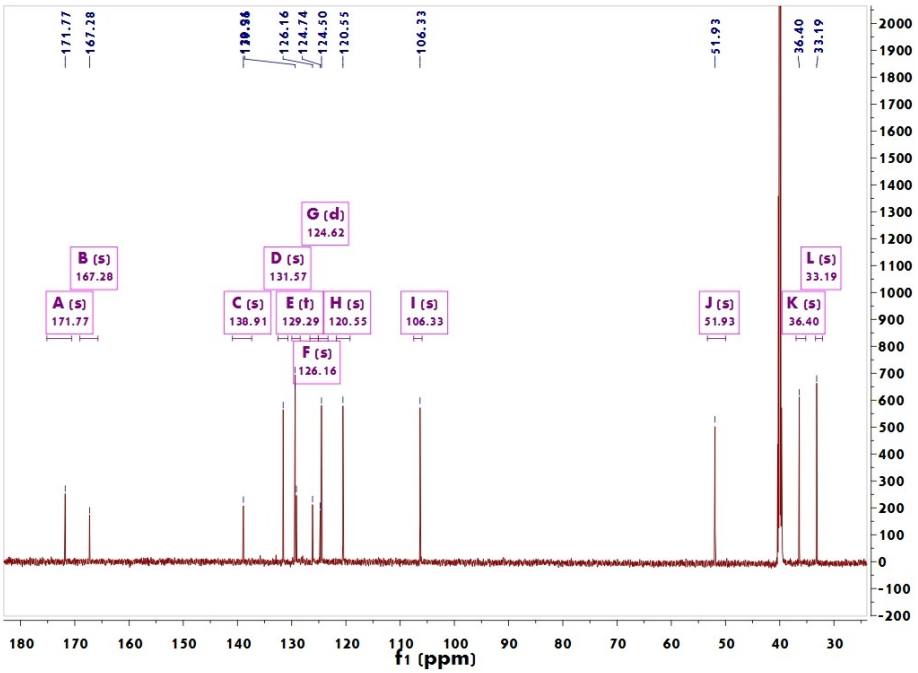

Fig. S2. ^{13}C-NMR spectra of compound 1'.

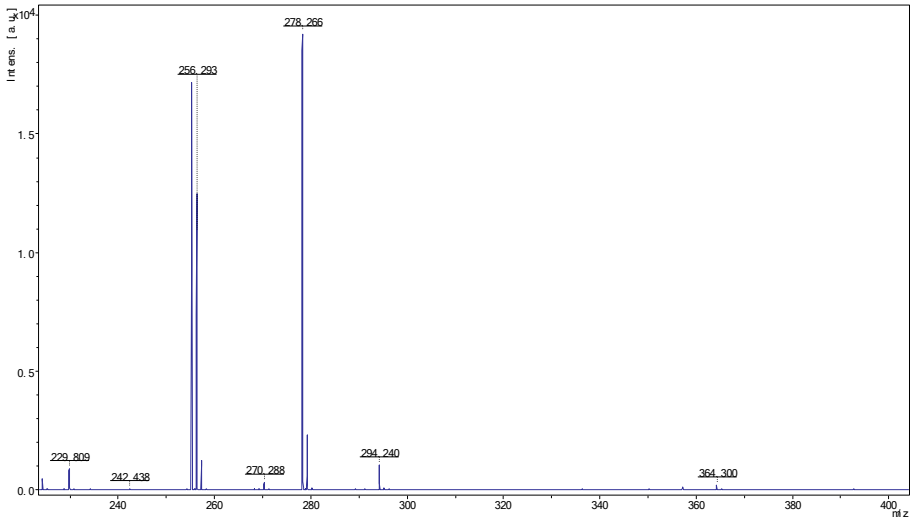

Fig. S3. MALDI-TOF mass spectrometry of compound 1'.

Synthesis of compound 2'. Compound 1' (1.35 g, 5.0 mmol) was dissolved in tetrahydrofuran (40 mL) under nitrogen and with constant stirring followed by addition of methylmagnesium chloride (3.0 M solution in tetrahydrofuran, 13.4 mL, 40 mmol). With constant stirring, the solution was refluxed for 2 hours. Then the mixture was added dropwise to a cooled solution of 1 M hydrochloric acid for 1 hour. After KPF_6 (0.92 g, 5.0 mmol) was added dropwise into the solution with constant stirring at room

temperature for 6 hours. The precipitate produced was filtered under suction to afford light green solid as crude product without further purification for next reactions.

Synthesis of compound 3'. Compound 2-chloro-3-(hydroxymethylene)cyclohex-1 -enecarbaldehyde was prepared according to the literature reported. Compounds 2' (0.80 g, 1.9 mmol) and 2-chloro-3-(hydroxymethylene)cyclohex-1-enecarbaldehyde (0.15 g, 0.86 mmol) were dissolved in acetic anhydride (30 mL) under nitrogen, followed by the addition of sodium acetate (0.16 g, 2.0 mmol). The mixture was stirred at room temperature for 4 hours. The solution was concentrated under reduced pressure to give dark red oil, which was purified by column chromatography using dichloromethane/methanol (50:1, v/v) as the eluent to afford compound 3' as dark red solid with a yield of 53% (0.38 g).

^{1}H-NMR (d_6-DMSO, 400 MHz, ppm) δ = 8.57 (d, J = 8.4 Hz, 2H), 8.22 (d, J = 7.2 Hz, 2H), 7.99 (t, J = 7.8 Hz, 2H), 7.67-7.62 (m, 4H), 7.55 (t, J = 7.8 Hz, 2H), 7.23-7.17 (m, 4H), 5.34 (s, 4H), 3.61 (s, 6H), 2.70 (t, J = 7.2 Hz, 2H), 2.50 (t, J = 7.2 Hz, 2H), 1.98-1.89 (m, 4H), 1.63-1.56 (m, 2H). MALDI-MS: Calcd. For $C_{40}H_{36}ClN_2O_4^+$ [M^+] 643.236, *found*: 643.392.

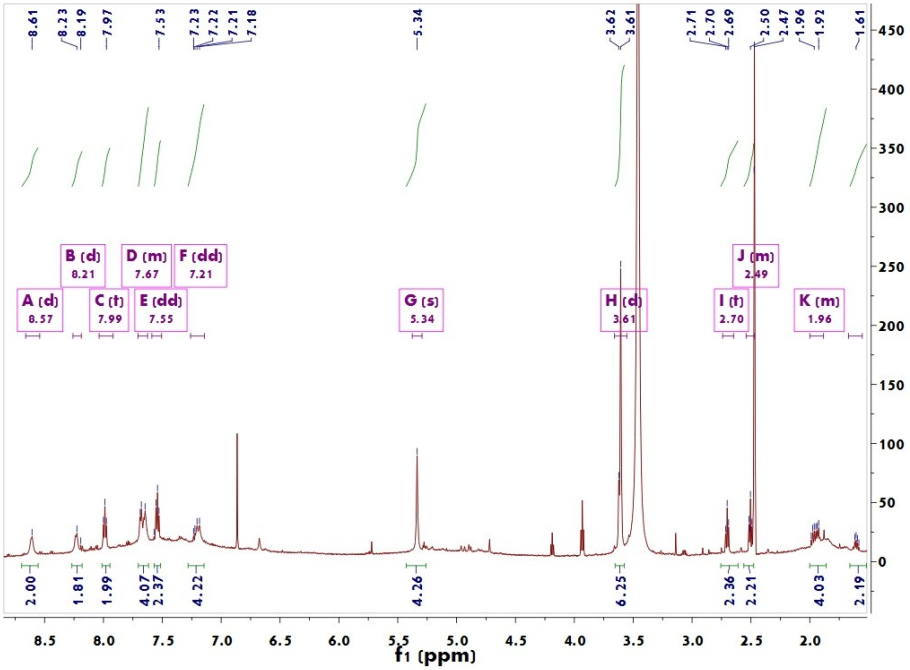

Fig. S4. ^{1}H-NMR spectra of compound 3'.

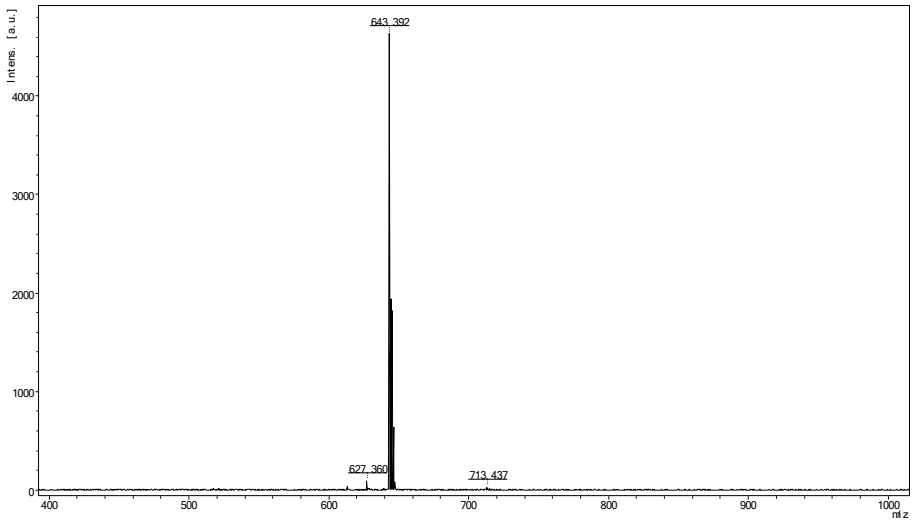

Fig. S5 MALDI-TOF mass spectrometry of compound 3'.

Synthesis of compound MT. Compounds 3' (0.017 g, 0.02 mmol) and 4-mercaptophenol (0.013 g, 0.1 mmol) were dissolved in N,N-dimethyformamide (10.0 mL) under nitrogen, the solution was stirred at room temperature for 4 hours. The solution was concentrated under reduced pressure to give dark solid, which was purified by column chromatography using dichloromethane/methanol (50:1, v/v) as the eluent to afford compound MT as dark red solid with a yield of 35% (0.007 g).

^{1}H-NMR (d_6-DMSO, 400 MHz, ppm) δ = 9.03 (d, *J* = 10.8 Hz, 2H), 8.22-8.06 (m, 4H), 7.87 (t, *J* = 7.8 Hz, 2H), 7.70 (d, *J* = 7.2 Hz, 2H), 7.59 (t, *J* = 7.8 Hz, 2H), 7.42-7.34 (m, 2H), 7.19 (d, *J* = 7.2 Hz, 2H), 6.70 (t, *J* = 8.4 Hz, 4H), 5.28 (s, 1H), 4.06 (s, 4H), 3.48 (s, 6H), 2.92-2.78 (m, 4H), 2.05-1.98 (m, 2H), 1.78 (t, *J* = 6.0 Hz, 4H). MALDI-MS: Calcd. For $C_{46}H_{41}N_2O_5S^+$ [M^+] 733.274, *found*: 733.486.

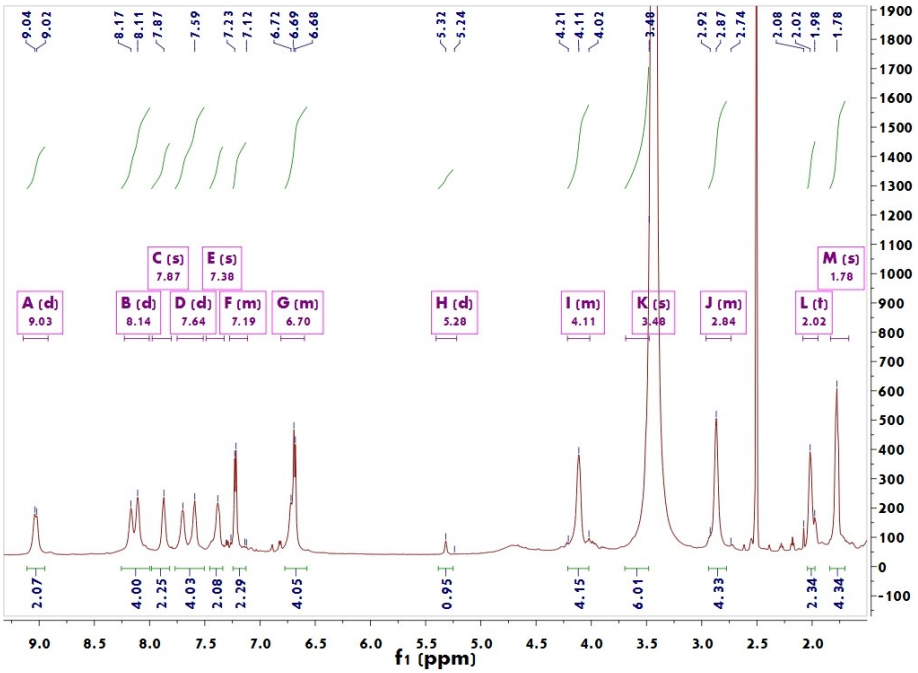

Fig. S6 ^{1}H-NMR spectra of compound MT.

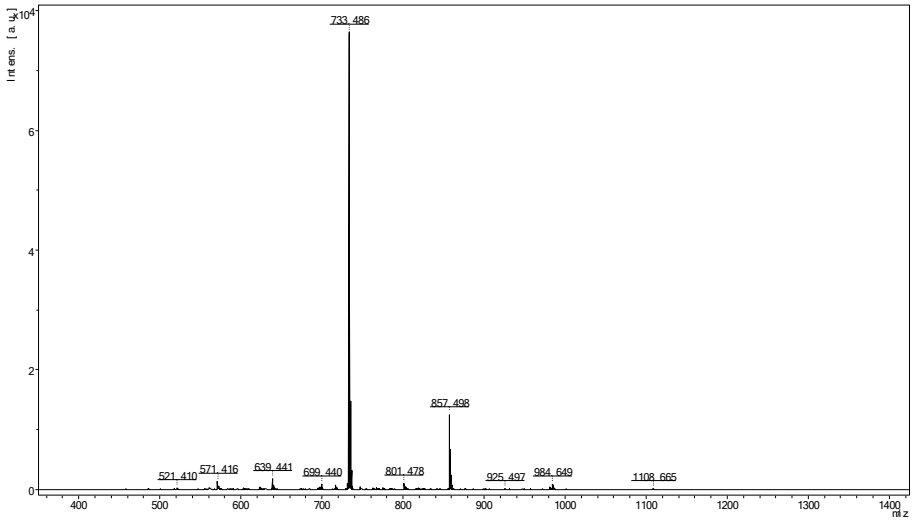

Fig. S7 MALDI-TOF mass spectrometry of compound MT.

Synthesis of compound 1. Compounds benzo[cd]indol-2(1H)-one (1.69 g, 10.0 mmol) and 3-bromoprop-1-yne (3.57g, 30.0 mmol) were dissolved in N,N- dimethyformamide (50.0 mL) under nitrogen and with constant stirring, the solution was refluxed for 6 hours. Then the mixture was poured into a large amount of ice water and adjusted to pH 7~8 with 1 M hydrochloric acid solution. The precipitate produced was filtered under suction, which was further purified by column chromatography using

dichloromethane as the eluent to give compound 1 as yellow solid with a yield of 72% (1.50 g).

^{1}H-NMR (d_6-DMSO, 600 MHz, ppm) δ = 8.18 (d, *J* = 8.1 Hz, 1H), 8.06 (d, *J* = 7.0 Hz, 1H), 7.79 (t, *J* = 7.8 Hz, 1H), 7.65 (d, *J* = 8.4 Hz, 1H), 7.56 (dd, *J* = 8.2, 7.3 Hz, 1H), 7.23 (d, *J* = 7.1 Hz, 1H), 4.73 (s, 2H), 3.28 (s, 1H). ^{13}C-NMR (d_6-DMSO, 100 MHz, ppm) δ = 166.56, 138.07, 131.86, 130.37, 129.51, 129.31, 129.13, 125.67, 124.85, 120.94, 106.71, 79.19, 74.90, 29.44. MALDI-MS: Calcd. For $C_{14}H_{10}NO^{+}$ [M+H^{+}] 208.076, *found*: 208.170.

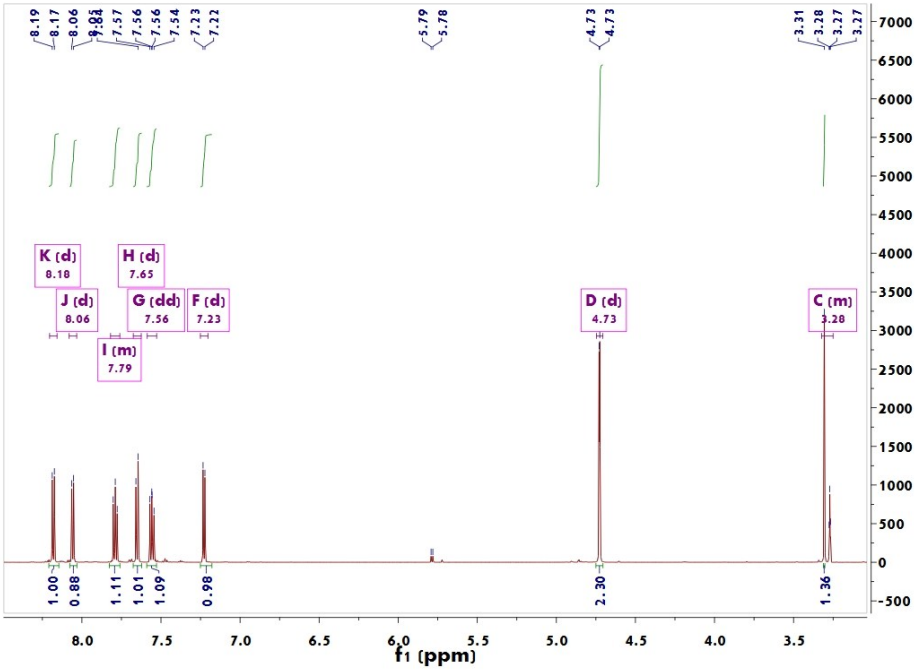

Fig. S8 ^{1}H-NMR spectra of compound 1.

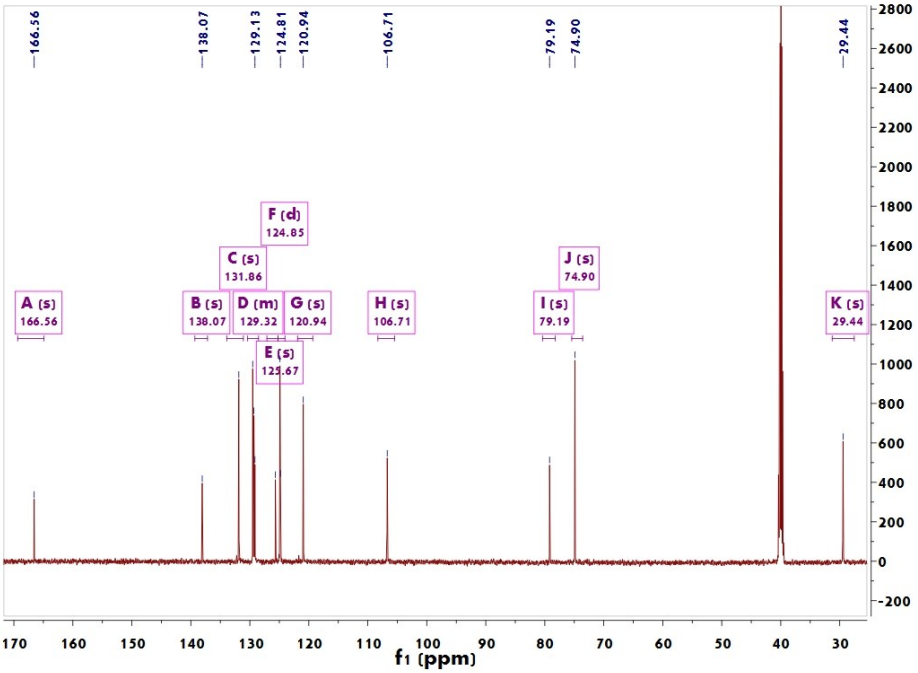

Fig. S9 ^{13}C-NMR spectra of compound 1.

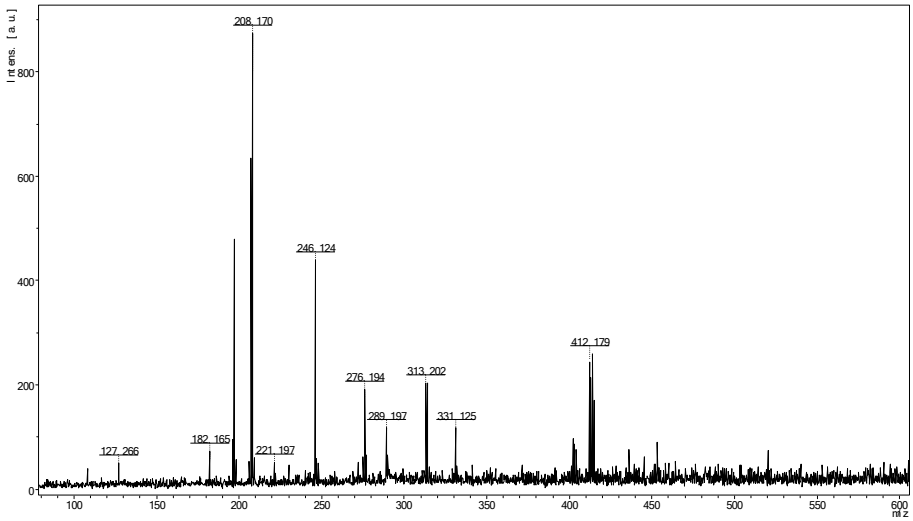

Fig. S10 MALDI-TOF mass spectrometry of compound 1.

Synthesis of compound 2. Compound 1 (1.03 g, 5.0 mmol) were dissolved in tetrahydrofuran (40 mL) under nitrogen and with constant stirring followed by addition of methylmagnesium chloride (3.0 M solution in tetrahydrofuran, 13.4 mL, 40 mmol). With constant stirring, the solution was refluxed for 2 hours. Then the mixture was added dropwise to a cooled solution of 1 M hydrochloric acid for 1 hour. After KPF_6 (0.92 g, 5.0 mmol) was added dropwise into the solution with constant stirring at room

temperature for 6 hour. The precipitate produced was filtered under suction to afford light green solid as crude product without further purification for next reactions.

Synthesis of compound 3. Compounds 2 (0.77 g, 2.19 mmol) and 2-chloro-3-(hydroxymethylene)cyclohex-1-enecarbaldehyde (0.17 g, 0.98 mmol) were dissolved in acetic anhydride (30.0 mL) under nitrogen, followed by the addition of sodium acetate (0.16 g, 1.95 mmol). The mixture was stirred at room temperature for 4 hours. The solution was concentrated under reduced pressure to give dark red oil, which was purified by column chromatography using dichloromethane/methanol (50:1, v/v) as the eluent to afford compound 3 as dark red solid with a yield of 63% (0.44 g).

^{1}H-NMR (d_6-DMSO, 400 MHz, ppm) δ = 8.55 (d, J = 14.4 Hz, 2H), 8.36-8.10 (m, 4H), 7.88 (t, J = 7.2 Hz, 2H), 7.70-7.54 (m, 4H), 7.43 (s, 2H), 6.69 (d, J = 7.8 Hz, 2H), 4.17 (s, 4H), 2.85-2.74 (m, 4H), 1.93 (s, 2H), 1.78 (s, 2H). MALDI-MS: Calcd. For $C_{38}H_{28}ClN_2^+$ [M^+] 547.194, *found*: 547.260.

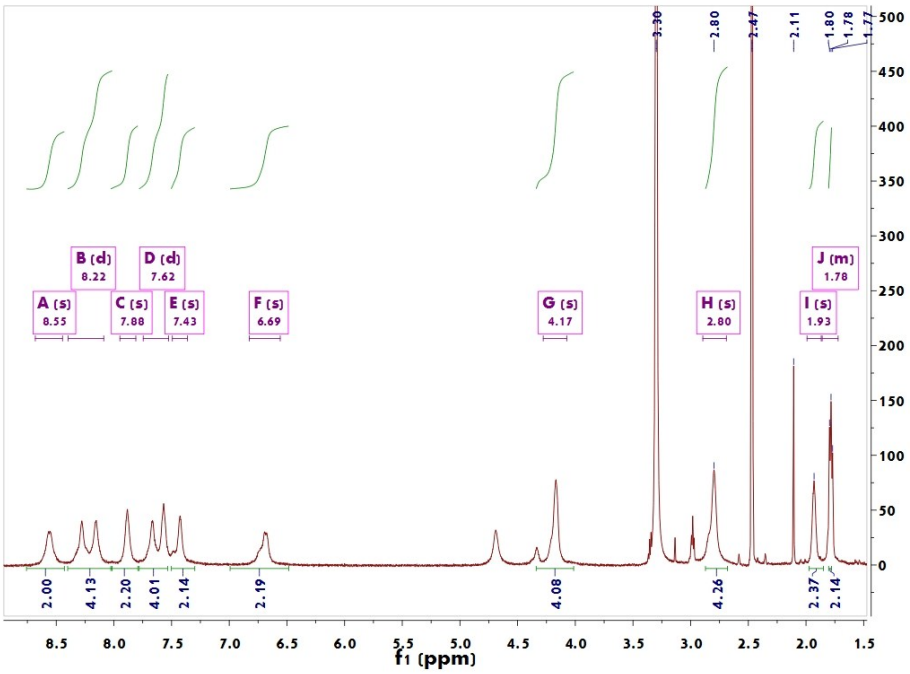

Fig. S11 ^{1}H-NMR spectra of compound 3.

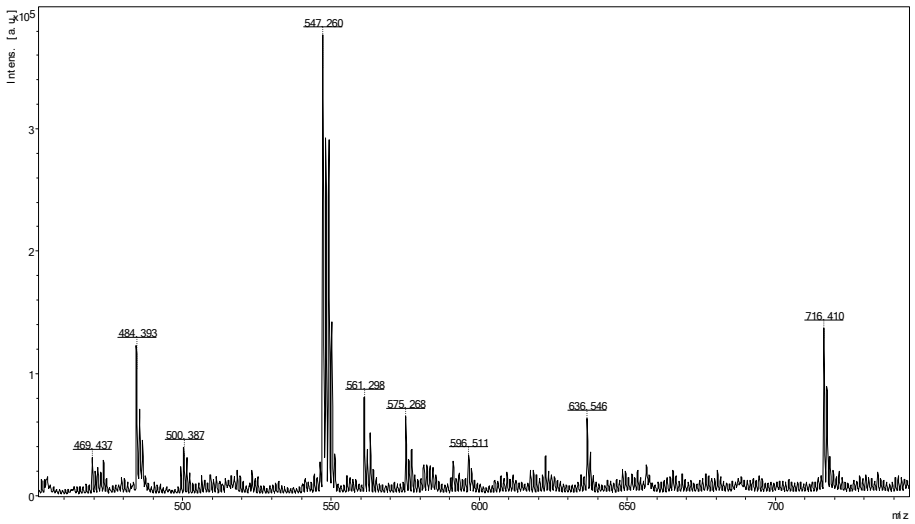

Fig. S12 MALDI-TOF mass spectrometry of compound 3.

Synthesis of compound 4. Compounds 3 (0.035 g, 0.05 mmol) and 4-mercaptophenol (0.032 g, 0.25 mmol) were dissolved in N,N-dimethyformamide (10.0 mL) under nitrogen, the solution was stirred at room temperature for 4 hours. The solution was concentrated under reduced pressure to give dark solid, which was purified by column chromatography using dichloromethane/methanol (50:1, v/v) as the eluent to afford compound 4 as dark red solid with a yield of 56% (0.022 g).

^{1}H-NMR (d_6-DMSO, 400 MHz, ppm) δ = 8.40 (d, J = 7.2 Hz, 3H), 8.22-7.99 (m, 4H), 7.82 (t, J = 7.8 Hz, 3H), 7.58-7.41 (m, 4H), 7.38-7.26 (m, 2H), 6.69-6.40 (m, 4H), 5.31 (s, 1H), 3.97 (s, 4H), 2.87 (d, J = 9.0 Hz, 2H), 2.80-2.64 (m, 4H), 2.15-2.11 (m, 2H). MALDI-MS: Calcd. For $C_{44}H_{33}N_2OS^+$ [M^+] 637.2341, *found*: 637.318.

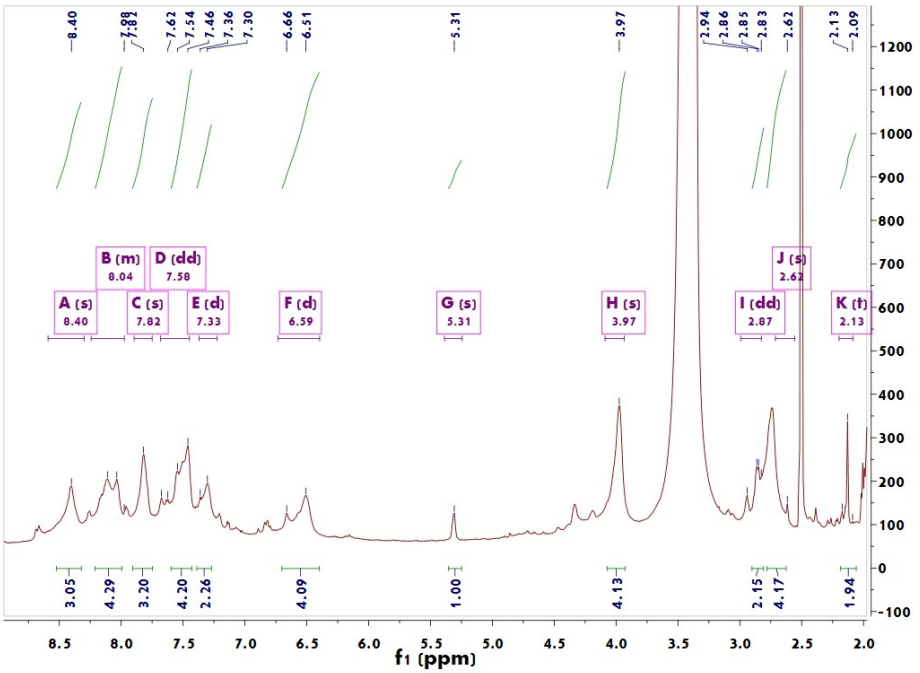

Fig. S13 ^{1}H-NMR spectra of compound 4.

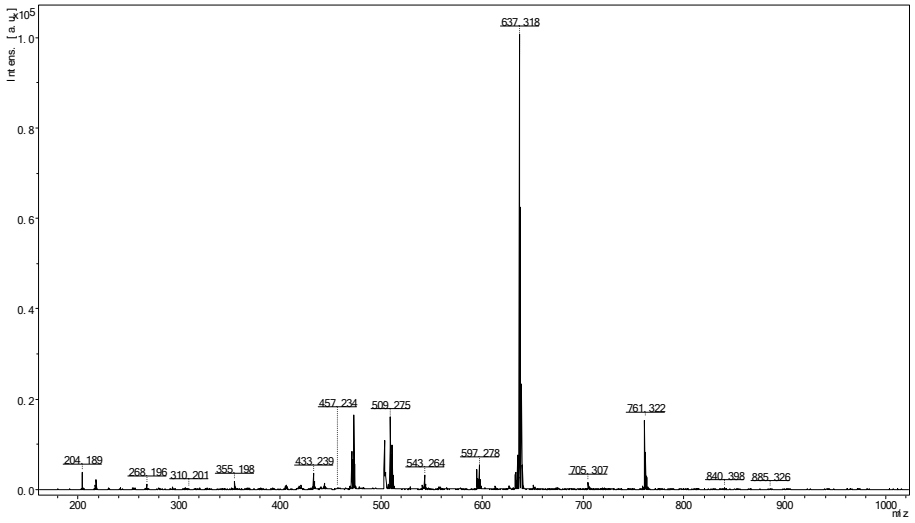

Fig. S14 MALDI-TOF mass spectrometry of compound 4.

Synthesis of compound QT-RGD. Compound 4 (7.83 mg, 0.01 mmol) was dissolved in dimethyl sulfoxide (10.0 mL) under nitrogen and with constant stirring, followed by the addition of cRGD-N_3 (19.38 mg, 0.03 mmol), $CuSO_4 \cdot 5H_2O$ (1.25 mg, 0.005 mmol) and sodium ascorbate (1.98 mg, 0.01 mmmol). The mixture was stirred at room temperature for 1 hour. Then the solution was concentrated under reduced pressure to yield black solid, which was purified by column chromatography using

dichloromethane/methanol (100:1 to 10:1, v/v) as the eluent, and QT-RGD was collected as dark red solid (4.63 mg, 24%). MALDI-MS: Calcd. For $C_{98}H_{111}N_{24}O_{17}S^+$ [M^+] 1928.831, *found*: 1928.816.

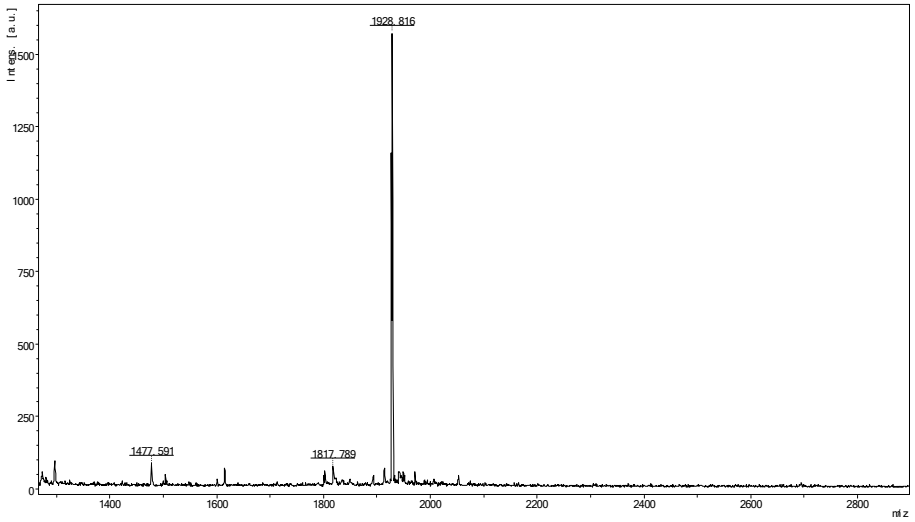

Fig. S15 MALDI-TOF mass spectrometry of QT-RGD.

4. NIR II fluorescence quantum yield

NIR II fluorescence quantum yields of the MT and QT-RGD were calculated following equation (1):

$$\Phi_s = \Phi_r\left(\frac{A_r\eta_s^2 D_s}{A_s\eta_r^2 D_r}\right) \quad (1)$$

The subscripts *s* and *r* stand for designate the sample and reference sample, respectively. A is the absorbance of samples at 808 nm, η is the average refractive index of the solution, and D is the integrated fluorescence area under the corrected emission spectrum. Here, standard NIR II dye IR-26 was used as the reference (Φ = 0.05%). All the measurements were at room temperature.

5. Cytotoxicity assay

4T1 cells (murine breast carcinoma) or NIH/3T3 cells (mouse embryonic fibroblast) growing in the log phase were seeded into 96-well plates (~1×10^4 cells/well) and allowed to adhere for 24 hours. MT or QT-RGD stock solutions were diluted by fresh

medium to the desired concentrations. The cell medium was then exchanged by new medium with different concentrations of MT or QT-RGD. After 24 hours incubation at 37°C in 5% CO_2, the cell viability was measured by MTT assay. The cell medium was subsequently replaced by 100 μL of fresh cell culture medium followed by addition of MTT solution (10 μL, 5 mg/mL) into each well. The cells were further incubated at 37°C for 4 hours in 5% CO_2. The absorbance of assays was measured at 450 nm. The absorbance measured for an untreated cell population under the same experimental condition was used as the reference point to establish 100% cell viability. A micro-plate reader (Thermo, Varioskan Flash) was used to measure the absorption of each solution. Duplicated experiments have been tested.

6. Mice tumor model

All animal studies were performed in strict accordance with the Guidelines for Care and Use of Laboratory Animals of Soochow University (Suzhou, China) and was approved by the Animal Ethics Committee of the Soochow University Laboratory Animal Center (Suzhou, China). The five-week-old female BALB/c mice with body weights of 14-16 g were purchased from Chang Zhou Cavensla Experimental Animal Technology Co. Ltd.

The mice were housed under standard conditions (25 ± 2°C, 60% ± 10% relative humidity) with 12 hours light/dark cycle. The tumors were grafted by injection of 3×10^6 4T1 cells in 50 μL of PBS into the back of each mouse. Tumors were allowed to grow to 4 mm in diameter for the imaging studies.

7. Blood circulation behavior

For in vivo pharmacokinetic studies, healthy BALB/c mice (n = 4) were intravenously injected with the MT and QT-RGD. Blood samples were drawn from their eye sockets at different time points of post injection, i.e., 3 min, 15 min, 30 min, 1 h, 2 h, 4 h, 6 h, 8 h, 12 h, 24 h and 48 h, respectively. Then the blood samples were weighed, and the radioactivity was measured by a γ counter (Multi Crystal LB 2111 γ Counter).

8. Biodistribution studies

For the ex vivo biodistribution study, 4T1 tumor-bearing mice (n = 3) were intravenously injected with MT or QT-RGD (100 μM, 200 μL). After being sacrificed at 6 h, tumor tissues and major organs including heart, liver, spleen, lung and kidneys were collected and weighed. The tissues were homogenized in PBS buffer (pH = 7.4) for 3 min, and then freeze-dried in vacuo overnight. After that, the tissue samples were dissolved in dimethylsulfoxide and centrifuged the solution. The NIR-II fluorescence emission spectra were conducted by collecting the supernatant. The %ID/g was calculated for comparison.

9. NIR II fluorescence imaging

In vitro and in vivo NIR II fluorescence imaging was performed with a Serious II 900-1700 nm NIR II Imaging System. For in vitro NIR II fluorescence imaging, centrifuge tubes containing the MT and QT-RGD solution (10 μM, 200 μL) were illuminated with 42 mW cm^{-2} of light from 808 nm laser. For in vivo NIR II fluorescence imaging, mice were firstly anesthetized with 3% isoflurane mixed with oxygen gas (0.5 L/min). After pre-contrast images were collected, the mice were intravenously injected with the MT (100 μM, 200 μL), QT-RGD (100 μM, 200 μL), followed by the acquisition of NIR II fluorescence images with 68 mW cm^{-2} of light from 808 nm laser at different time points. All NIR II fluorescence images were collected with an exposure time of 200 ms.

10. Photoacoustic imaging

In vitro and in vivo photoacoustic (PA) imaging experiments were assessed by the real-time multispectral optoacoustic tomography system (MSOT, iThera Medical GmbH, inSight/inVision 256). The laser system with tunable wavelength (680-980 nm, 10 Hz repetition rate, 8 ns pulse interval, 120 mJ pulse peak energy) was used to excite the target object with optical pulses to generate the PA effect. The phantom is made of polyurethane, specially designed to mimic the shape, size, and optical properties of a mouse, containing two inner cylindrical channels for holding the control medium (Milli-Q water) and the contrast agent solution.

For in vitro PA imaging, the excitation wavelength of 808 nm was adopted. For in vivo PA imaging, mice were firstly anesthetized with 3% isoflurane mixed with oxygen gas (0.5 L/min). Subsequently, the solutions of MT and QT-RGD (100 μM, 200 μL) were injected to mice via the tail vein after pre-contrast images collected. Then the mice were placed into a water bath to maintain their body temperature at 37°C for following tumor imaging. There are two groups of mice (three mice per group). PA signal intensities in the region of interest (ROI) were measured using the MSOT imaging system software package.

11. Photothermal Performance

For in vitro photothermal performance, different concentrations of aqueous solutions of MT or QT-RGD were irradiated under an 808 nm laser with a power density of 1 W cm^{-2} for 10 min. And the aqueous solutions of MT or QT-RGD with the different power density were also investigated. The temperature was measured via an infrared thermal imaging instrument (FLIR, A65). And the photostability was tested by five cycles of irradiating and cooling processes. The photothermal conversion efficiency (η) was calculated using the following equations (2):

$$\eta = \frac{m \cdot c \cdot (T_{max} - T_{max \cdot H_2O})}{I \cdot (1 - 10^{-A}) \cdot \tau_S} \quad (2)$$

where m is the solution mass, c is the heat capacity of water (4.2 J/g), T_{max} and $T_{max \cdot H2O}$ are maximum temperatures achieved in the presence or absence of the MT or QT-RGD, respectively. I is the laser power density (1 W cm^{-2}), A is the absorbance of the aqueous solutions of MT or QT-RGD at 808 nm, and τ_s is system time constant.

For photothermal ablation of cancer cells, 4T1 cells were seeded in 12-well plates with a density of 5×10^4 cells/well. After 24 h of growing, cells were incubated with the different concentrations of MT or QT-RGD (2, 4, 8 and 16 μM) for 4 h. Then the cells were received 808 nm laser irradiation (1 W cm^{-2}, 5 min). The cells receiving different treatments were stained with live/dead staining kit and observed with fluorescence microscope. The live cells appeared green, while the dead ones were red.

The photothermal ablation effect of MT or QT-RGD was further evaluated through

MTT analysis. 4T1 cells were planted in 96-well plates with a concentration of 5×10^3 cells/well. After growing for 24 h, they were subjected to different treatments as mentioned above and analyzed through MTT assay.

For in vivo infrared thermal imaging, the aqueous solutions of QT-RGD (100 μM, 200 μL) were intravenously injected into the mice bearing 4T1 tumors. The tumors were irradiated for 10 min using an 808 nm laser (1 W cm^{-2}) at 4 h post-injection, and the full-body images were simultaneously captured using an infrared camera (FLIR, A65) during the irradiation.

For in vivo photothermal therapy, 4T1 tumor-bearing BALB/c mice (20 mm^3) were randomly divided into six groups (n = 5): mice injected with PBS (group 1, PBS), mice treated with 808 nm laser irradiation after PBS injection (group 2, PBS+808 nm), mice injected with QT-RGD (group 3, QT-RGD), mice treated with 808 nm laser irradiation after MT injection (group 4, MT+808 nm), mice treated with 808 nm laser irradiation after c-RGD and QT-RGD injection (group 5, cRGD+QT-RGD+808 nm), and mice treated with 808 nm laser irradiation after QT-RGD injection (group 6, QT-RGD+808 nm). Note that the above agents were intravenously injected, and all therapeutic irradiations were applied 4 h post-injection. The power density of 808 nm laser was 1 W cm^{-2} and the exposure time was 10 min. Tumor size was measured with a caliper and tumor volume was calculated every other day as follows: $V = L\cdot W^2/2$, where W and L are the widest and longest dimensions of the tumor, respectively. The tumor volumes were normalized against the original volumes at 0 day for monitoring the tumor growth. The tumor tissues were resected from the mice on 3 d post-treatment for evaluating the therapeutic efficacy of different treatments through pathological analysis.

12. Radio-iodination with Chloramine-T Method

MT or QT-RGD was dissolved in PBS buffer (100 μM, 200 μL, pH = 7.4), labeled with $Na^{125}I$ (1.2 mCi), and then chloramine-T in PBS (10 mg/mL, 10 μL, pH = 7.4) was added. The reaction mixture was incubated for 10 min with shaking at room temperature. The crude reaction was then passed over a C18-SepPak (pretreated first

with 95% EtOH and then 10 μM PBS), and the volume of the product was controlled at 50 μL. For imaging, the concentrate was further diluted in 200 μL of PBS.

13. In Vivo SPECT/CT Imaging

In vivo SPECT/CT imaging was performed on a micro SPECT/CT scanner (Milabs, Utrecht, the Netherlands) with a multipinhole focused collimator. The SPECT was performed for 15 min per scan with an energy window from 20 to 40 KeV. The parameter of the CT scan was set as an accurate mode using three frames averaging, full angle, with 55 kV tube voltage and 615 mA tube current.

4T1 tumor bearing mice were injected with ^{125}I-MT or ^{125}I-QT-RGD (400 μCi) by intravenous injection without thyroid pre-blocking. The 3% isoflurane/oxygen gas mixture (flow rate: 0.5 L/min) was used to anesthetize the mice by inhalation on a temperature controlled animal bed of the micro SPECT/CT, scanned with varied times (1, 2, 4, 8, 12 and 24 h). All micro SPECT/CT data were handled with PMOD (version 3.602) software.

13. Supplementary Figures

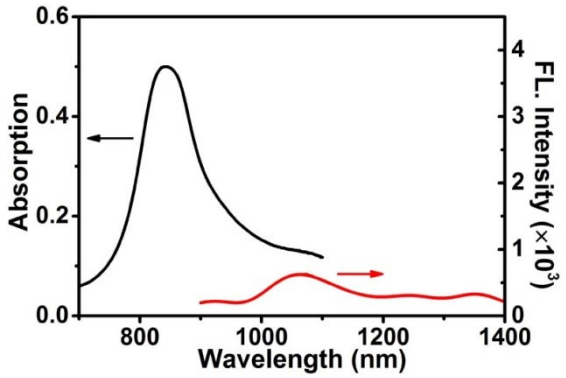

Fig. S16 Absorption and fluorescence spectra of the MT (5 μM) in water solution containing 5 % (V/V) DMSO.

Table S1 Quantum yield of MT, QT-RGD in DMSO solvent.

	IR26	MT	QT-RGD

QY(Φ)	0.05%	0.07%	0.12%

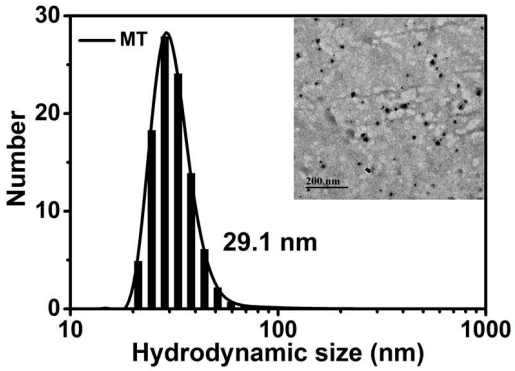

Fig. S17 The hydrodynamic size of MT (5 μM) in water solution. The inset is TEM image. Sacle bar: 200 nm.

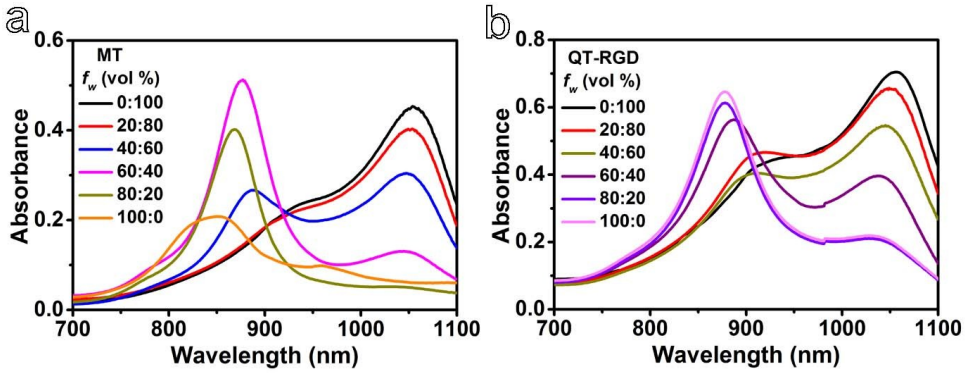

Fig. S18 Absorption spectra of the MT (a) and QT-RGD (b) in DMSO/water mixtures (excited at 808 nm).

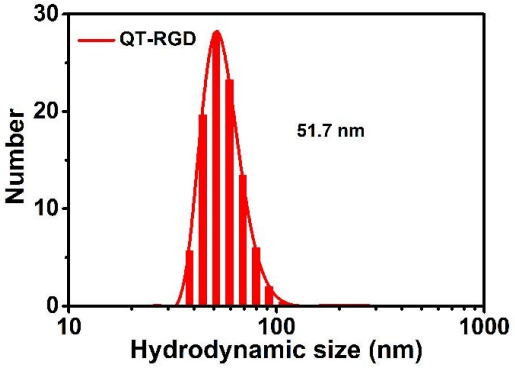

Fig. S19 The hydrodynamic size of QT-RGD (5 μM) in water solution.

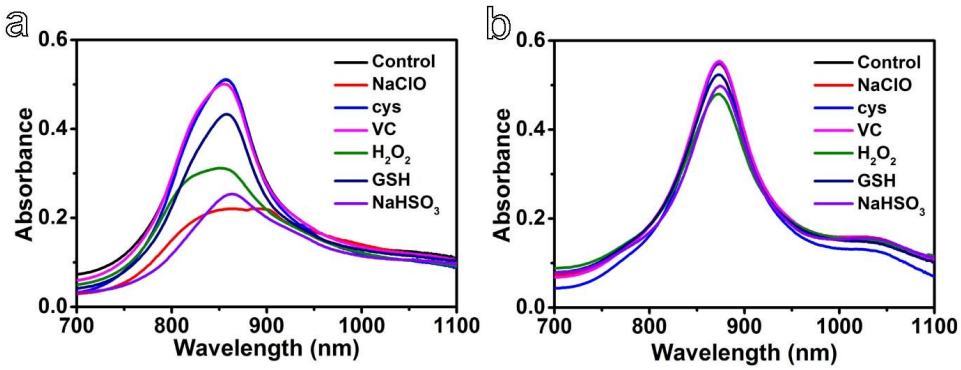

Fig. S20 (a) Fluorescence spectra of the MT (5 μM) treated with different interfering species (10 equiv.) in water solvents (excited at 808 nm). (b) Fluorescence spectra of the QT-RGD (5 μM) treated with different interfering species (10 equiv.) in water solvents (excited at 808 nm).

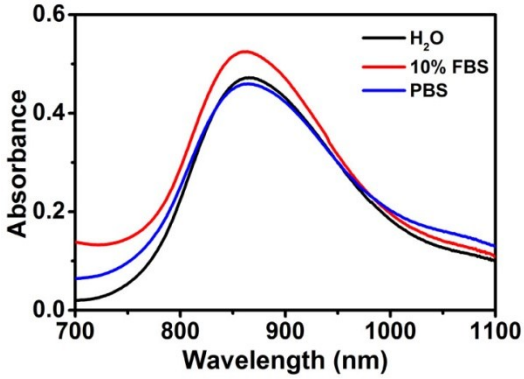

Fig. S21 Absorption spectra of QT-RGD in H_2O, 10% FBS solution or PBS buffer after 0.5 h incubation.

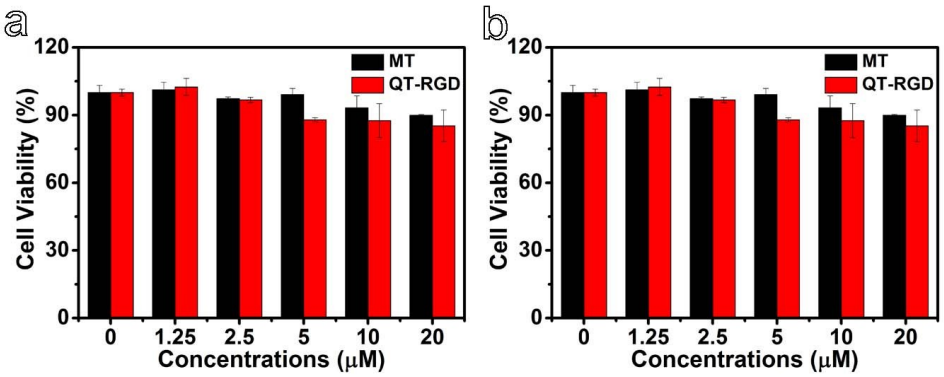

Fig. S22 (a) MTT assays on the viability of 4T1 cells after 24 h incubated with the different concentrations probes MT and QT-RGD, i.e., 0, 1.25, 2.5, 5, 10 and 20 μM (the error bars represent standard deviations of six parallel measurements). (b) MTT assays on the viability of 3T3 cells after 24 h incubated with the different concentrations probes MT and QT-RGD, i.e., 0, 1.25, 2.5, 5, 10 and 20 μM (the error bars represent standard deviations of six parallel measurements).

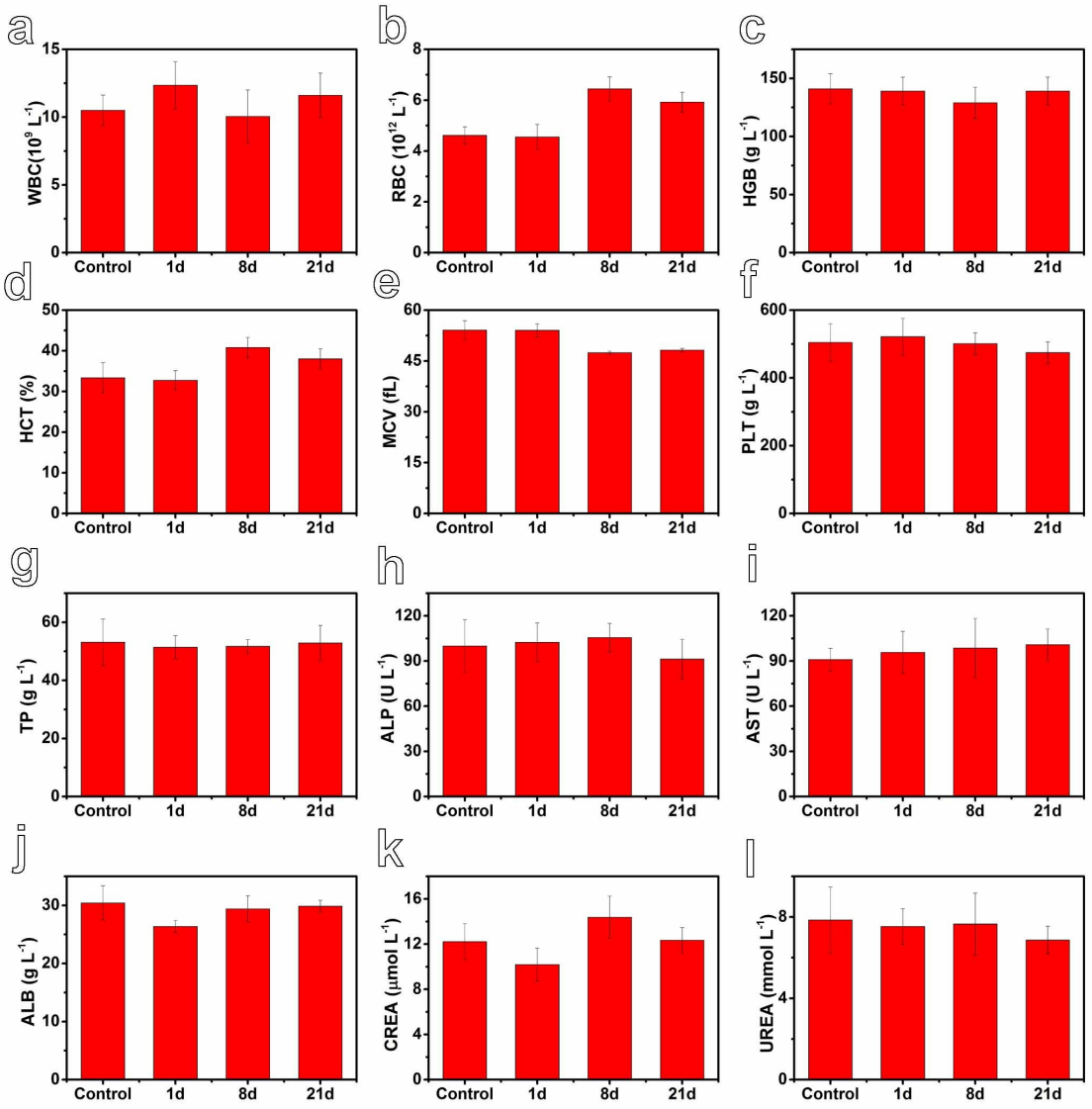

Fig. S23 Hemanalysis of BALB/c mice intravenously injected with MT-RGD blood routine test including (a) white blood cell count (WBC), (b) red blood cell count (RBC), (c) hemoglobin (HGB), (d) hematocrit (HCT), (e) mean corpuscular volume (MCV), (f) platelets (PLT); blood biochemical tests including (g) total protein (TP), (h) alkaline phosphatase (ALP), (i) aspartate aminotransferase (AST), (j) albumin (ALB), (k) creatinine (CREA), (l) urea nitrogen (UREA).

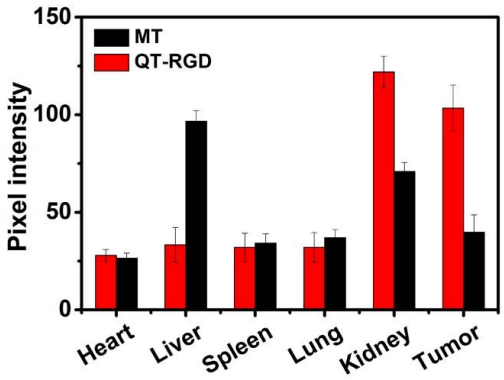

Fig. S24 Pixel intensity of main organs and tumors of MT and QT-RGD.

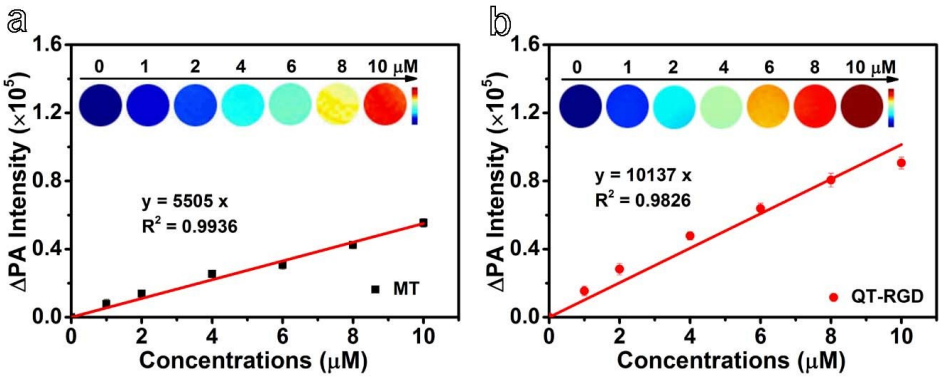

Fig. S25 (a) Linearity curve of ΔPA versus concentration of the MT in the range of 0-10 μM. (b) Linearity curve of ΔPA versus concentration of the QT-RGD in the range of 0-10 μM.

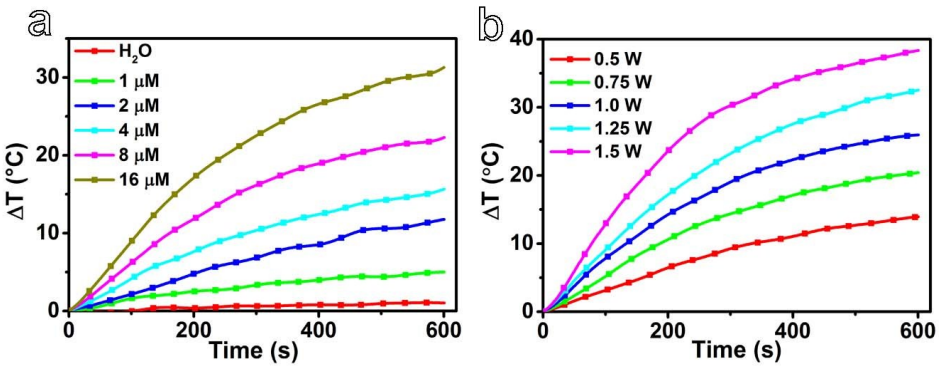

Fig. S26 (a) Temperature variation curves of QT-RGD with different concentrations under laser irradiation at 808 nm (1 W cm^{-2}). (b) Temperature variation curves of QT-RGD (16 μM) with different powers.

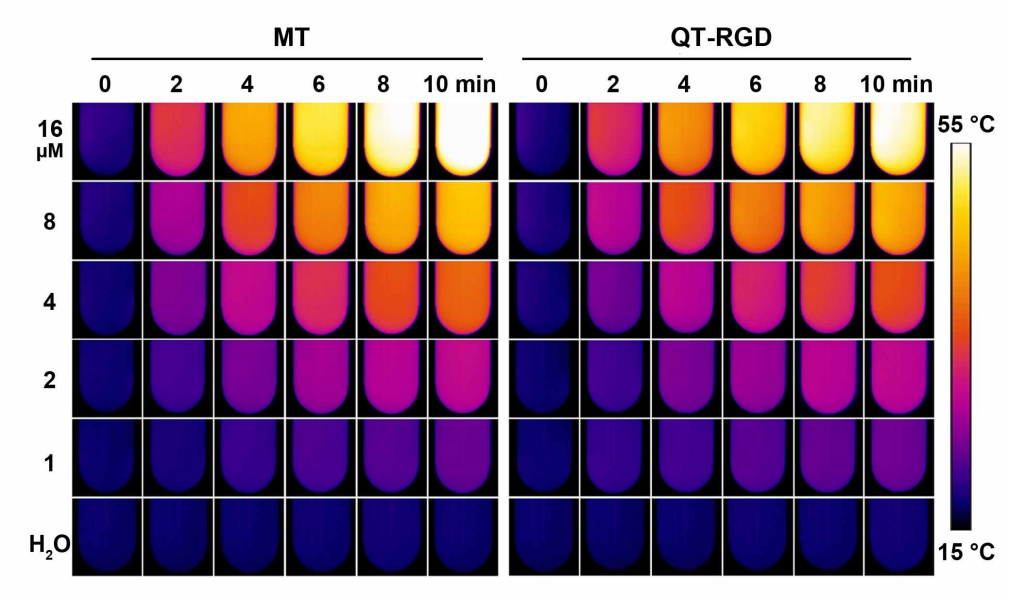

Fig. S27 Infrared thermal images of MT and QT-RGD with different concentrations at various time under laser irradiation at 808 nm (1 W cm^{-2}).

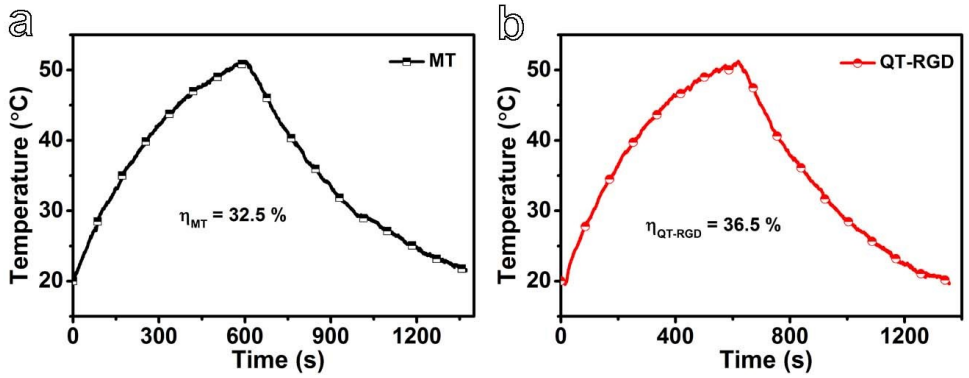

Fig. S28 (a) Heating and cooling profiles of the MT (16 μM) in water solution under an 808 nm laser with a power density of 1 W cm^{-2}. (b) Heating and cooling profiles of the QT-RGD (16 μM) in water solution under an 808 nm laser with a power density of 1 W cm^{-2}.

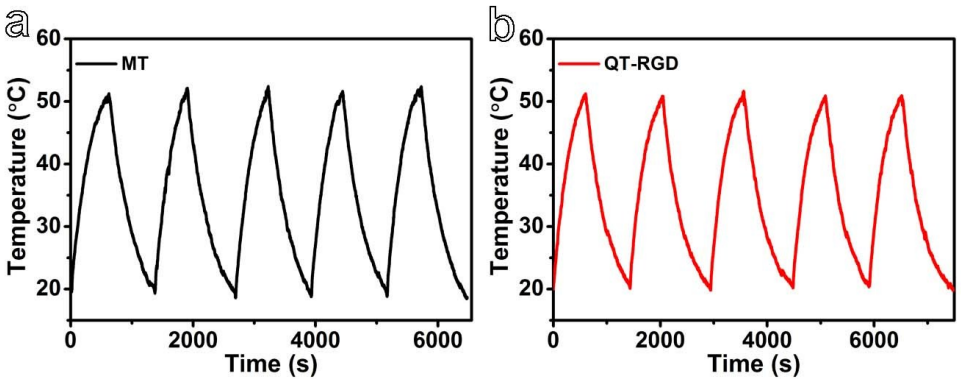

Fig. S29 (a) Heating and cooling cycles of the MT (16 μM) in water solution under an 808 nm laser with a power density of 1.0 W cm^{-2}. (b) Heating and cooling cycles of the QT-RGD (16 μM) in water solution under an 808 nm laser with a power density of 1 W cm^{-2}.

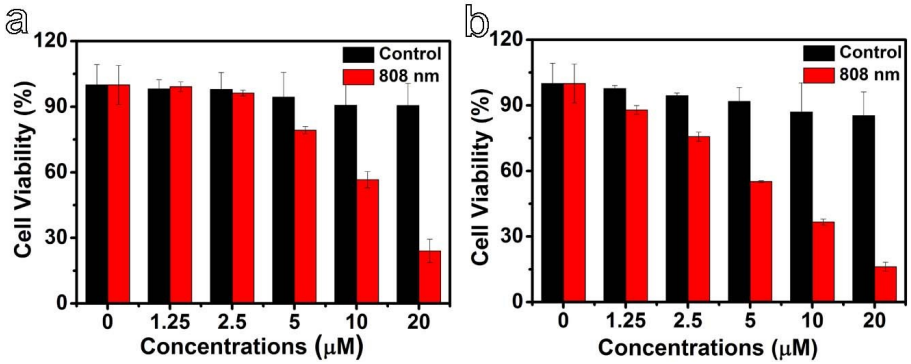

Fig. S30 (a) Cytotoxicity data results of 4T1 cells of the different concentrations MT (0, 1.25, 2.5, 5, 10 and 20 μM) with or without 808 nm laser irradiation obtained from the MTT assay (1 W cm^{-2}, 5 min). (b) Cytotoxicity data results of 4T1 cells of the different concentrations QT-RGD (0, 1.25, 2.5, 5, 10 and 20 μM) with or without 808 nm laser irradiation obtained from the MTT assay (1 W cm^{-2}, 5 min).

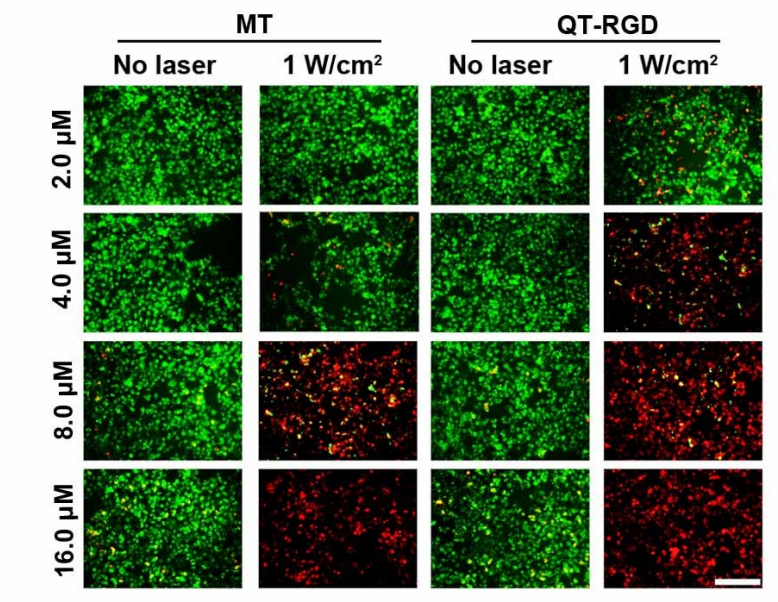

Fig. S31 Fluorescence images of 4T1 cells stained with live/dead kit of the different concentrations MT and QT-RGD (2, 4, 8 and 16 μM) after 24 h co-incubation for the thermal ablation effects. Scale bar: 200 μm.

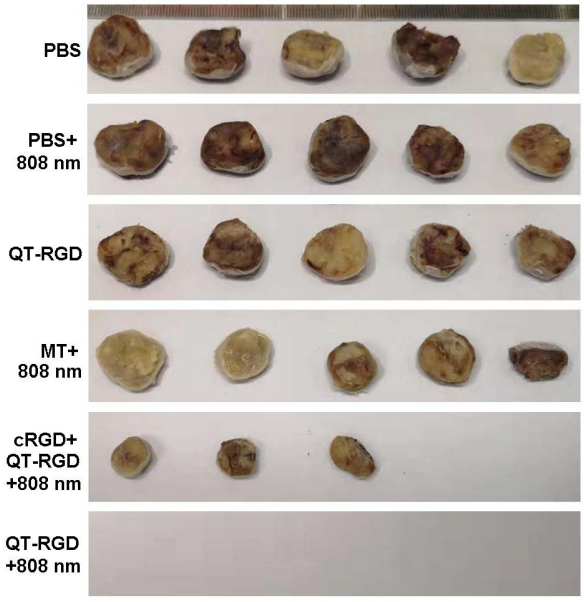

Fig. S32 Images of representative tumors taken from mice in different treatment groups.

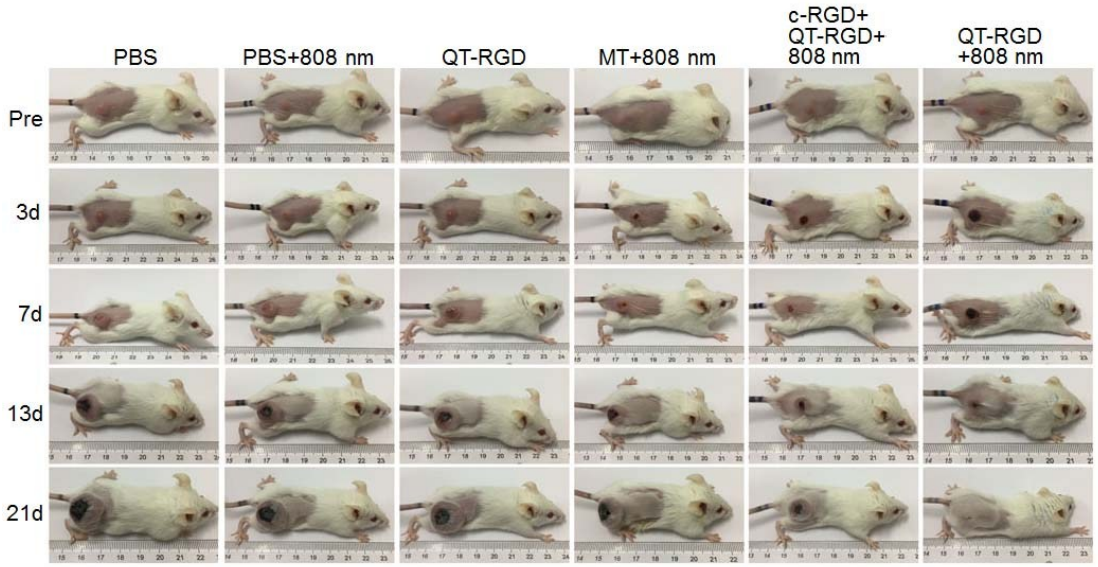

Fig. S33 Images and of representative mice captured on different days after each treatment.

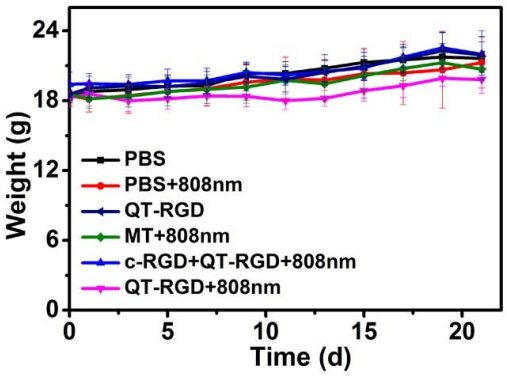

Fig. S34 Body weight changes of mice for each treatment group (n = 5).

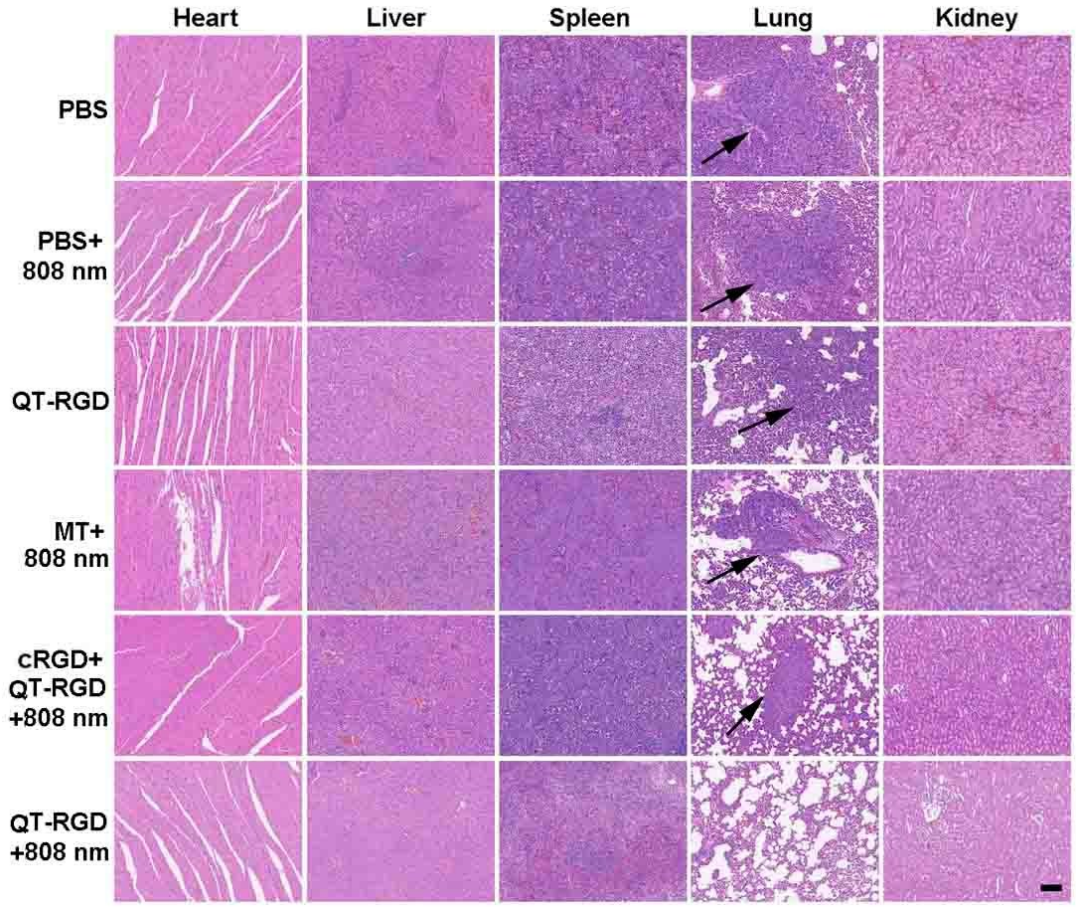

Fig. S35 H&E staining in main organs of representative mice captured on 21 days after each treatment. Scale bar: 500 μm.